Monovalent Cation Transport: Lack of Structural Deformation upon Cation Binding[†]

F. Tian, K.-C. Lee,[‡] W. Hu,[§] and T. A. Cross*

Center for Interdisciplinary Magnetic Resonance at the National High Magnetic Field Laboratory, Institute of Molecular Biophysics, and Department of Chemistry, Florida State University, Tallahassee, Florida 32306-4005

Received May 16, 1996; Revised Manuscript Received July 15, 1996[⊗]

ABSTRACT: Cations often deform the structure of regulatory proteins to affect a functional response, but for other protein functions a more passive effect is desired. For instance, it is shown here that in the conductance of Na^+ by the gramicidin channel there appears to be no significant structural deformation of either the side chains or backbone upon Na^+ binding in the channel. This is based on ^{15}N and ^{13}C chemical shifts, ^2H quadrupolar interactions, and $^{15}N-^2H$ dipolar interactions obtained by solid-state NMR spectroscopy of uniformly aligned lipid bilayer preparations of the gramicidin channel in the presence and absence of Na^+. This conclusion is despite some significant changes in the $^{15}N_\alpha$ and $^{13}C_1$ chemical shift values which are argued here to be the result of indirect polarization effects upon cation binding rather than reflections of structural and dynamic changes. The lack of structural deformation implies that Na^+ moves to the carbonyl oxygens lining the pore of this channel for solvation rather than the carbonyl groups moving in toward the channel axis. This forces the cations onto a helical path following the positions of the carbonyl oxygens around the channel pore. Furthermore, an ideal binding site geometry for Na^+ in the channel is avoided. Instead, adequate binding energy is provided by the channel to compensate for the loss of hydration energy when the cations enter the channel. The avoidance of strong binding ensures that efficient transport of the cations through the channel can be realized.

The binding of cations to a protein is often considered to be accompanied by structural deformation. However, a Ca^{2+} binding site in calbindin was recently shown to be "preformed"; i.e., the binding site geometry in the absence of cations was essentially the same as in the presence of Ca^{2+} (Skelton et al., 1994). For monovalent cation binding to proteins there is less structural information in the literature, but the atomic resolution crystal structure of the regulatory protein, dialkylglycine dicarboxylase, in the presence and absence of cations shows considerable structural change upon cation binding (Miller, 1993; Toney et al., 1993). No such atomic resolution structure is available for the proteinaceous monovalent cation channels. However, the binding of monovalent cations to cubic insulin crystals has been proposed as a model for cation binding in ion carriers and channels (Badger et al., 1994). While conformational changes occur upon cation binding in these crystals, the changes are discrete. Previously published results on the polypeptide cation channel, gramicidin A (gA),[1] suggested the possibility of significant conformational changes in the backbone structure (Smith et al., 1990; Ketchem et al., 1994; Separovic et al., 1994).

Gramicidin A is a linear polypeptide that as a dimer forms a transmembrane ion channel in lipid bilayers. This channel is a helix formed from a β-sheet type of secondary structure (Urry, 1971) resulting in a 4 Å diameter pore that supports a single file column of water molecules. This is made possible by the alternating D and L stereochemistry of the amino acids which orients all of the side chains on one side of the sheet, radiating toward the lipid environment. The high-resolution structure of gramicidin in a bilayer environment has been determined from orientation-dependent solid-state NMR data of samples uniformly aligned with respect to the magnetic field direction (Ketchem et al., 1993, 1994, 1996). When monovalent cations enter the gramicidin channel, all but two axial waters of hydration are stripped from the cation's hydration sphere, and it has been considered for decades that the carbonyl oxygens which line the channel pore provide the remaining solvation environment for these ions (Andersen, 1984; Urry, 1975; Jordan, 1990; Roux & Karplus 1993). Thallium ion binding sites near the channel mouth have been characterized by X-ray diffraction of oriented bilayers to be 9.6 Å from the bilayer center (Olah et al., 1991). In this symmetric dimer the binding of a cation to either monomer has the same affinity, but once a cation is bound, the symmetry is broken and the binding of a second cation to the other monomer is significantly weakened, hence the characterization of "strong" and "weak" binding constants (Hinton et al., 1986; Urry et al., 1982). For cations to pass through the channel, the single file column of water molecules in the pore translates with highly correlated motions (Mackay et al., 1984; Skerra & Brickmann, 1987; Chiu et al., 1989). These correlated motions extend to the polypeptide backbone lining the channel pore (Chiu et al., 1991; Elber et al., 1995; North & Cross, 1995), where they have been characterized as local librational amplitudes about the $C_\alpha-C_\alpha$ axis (Lazo et al., 1995). Such amplitudes (on the order of $\pm 20°$) suggest considerable flexibility that would

[†] This work has been supported by the National Institutes of Health (AI-23007).

[‡] Present address: Department of Chemistry and Biochemistry, University of Maryland, P.O. Box 223, College Park, MD 20742.

[§] Present address: Biophysics Research Division, University of Michigan, 930 North University, Ann Arbor, MI 48109-1055.

[⊗] Abstract published in *Advance ACS Abstracts,* September 1, 1996.

[1] Abbreviations: DMPC, dimyristoylphosphatidylcholine; HPLC, high-performance liquid chromatography; gA, gramicidin A; MD, molecular dynamics.

S0006-2960(96)01170-1 CCC: $12.00

allow for local ion-induced deformations of the backbone structure. However, amplitudes in just the nanosecond time scale consistent with cation translational motions are on the order of only ±6° (North & Cross, 1995).

Most of the functional models of the channel stem from detailed computational studies, and experimental verification has lagged behind. These models typically suggest substantial conformational changes upon cation binding that have the carbonyl oxygens swinging into the channel lumen so that four carbonyls and two water ligands solvate the cation (Aqvist & Warshel, 1989; Roux & Karplus, 1991; 1993; Roux, 1993). The conformational changes can be as large as 40° (Mackay et al., 1984; Venkatchalam & Urry, 1984) or smaller (Fischer & Brickmann, 1983; Jordan, 1990; Aqvist & Warshel, 1989; Roux & Karplus, 1991; Elber et al., 1995). Some of these models also suggest that it is not necessary to have four carbonyls to generate an adequate solvation environment (Fischer & Brickmann, 1983; Jordan, 1990; Elber et al., 1995), further suggesting a helical path for the cation through the channel. The sophistication of the MD calculations of gramicidin has escalated dramatically since the early 1980s when Hagler, Wilson, and co-workers were the first to use an all-atom model of gramicidin in their MD calculations (Mackay et al., 1984). Since then, aqueous solvation (Chiu et al., 1989), a molecular lipid environment (Woolf & Roux, 1994), and polarizability (Roux et al., 1995) have all been added among other complexities to these computations. Here, experimental evidence is presented that provides some structural detail for the cation−polypeptide interactions.

MATERIALS AND METHODS

Isotopically labeled amino acids were purchased from Cambridge Isotope Laboratories. Fmoc blocking chemistry was used, and solid-phase peptide synthesis was conducted on a Model 430A Applied Biosystems peptide synthesizer as described previously (Fields et al., 1989). By avoiding acid cleavage deuterated indole rings were successfully incorporated into the peptide. Peptides that were not greater than 98% pure were purified by HPLC using a semipreparative column (Fields et al., 1989).

Oriented samples were prepared by codissolving 20 mg of gramicidin and 60 mg of DMPC (1:8 molar ratio) in 5% methanol in benzene. Samples were dried once this solution was spread on thin glass slips and then hydrated with an aqueous solution to approximately 50% by weight water. The Na^+-loaded samples were prepared by hydrating with a 0.15 M NaCl solution for single occupancy and 2.4 M NaCl solution for double occupancy. The Na^+ binding constants were 36.9 M^{-1} for the stronger binding site (Hinton et al., 1986) and 2.6 M^{-1} for the weaker binding site (Urry et al., 1982). The cation occupancies were calculated as before (Smith et al., 1990; Separovic et al., 1994) from the addition of a known amount of Na^+ to these samples with a known binding constant for Na^+, but the occupancies will really reflect sodium ion activities which are very difficult to estimate in such samples. However, Na^+ does not interact strongly with phosphatidylcholine (Akutsu & Seelig, 1981) and the water content of these samples is near saturation levels, and therefore, the occupancy estimates as defined above are considered to be reasonable.

^{15}N NMR spectra were recorded with the bilayer normal parallel to B_o at an ^{15}N frequency of 40.58 MHz using cross polarization with a 5 μs 90° pulse width, 1 ms mixing time, and 35 μs Hahn echo delay. The chemical shift spectra were used to obtain not only the orientation-dependent chemical shifts but also the $^{15}N-^{2}H$ dipolar interaction. The ^{15}N chemical shift frequencies are given in parts per million relative to 0 ppm for a saturated solution of $^{15}NH_4NO_3$ or given on a kilohertz frequency scale relative to an arbitrary 0 point. ^{2}H spectra were obtained at 61.5 MHz using a quadrupole echo pulse sequence with a 1 μs dwell time, 2.8 μs 90° pulse width, and 30 μs echo delays. The NMR spectra were processed on a Silicon Graphics workstation using Felix software (Biosym/MSI). Molecular modeling was performed using Insight II software (Biosym/MSI).

RESULTS

Figure 1 shows both the ^{15}N chemical shift and $^{15}N-^{2}H$ dipolar interactions for $^{15}N_{\alpha,\epsilon 1}-Trp_{13}$-labeled gramicidin A in aligned lipid bilayers of DMPC. In Figure 1A the sample is fully protonated, and the protons are decoupled from the ^{15}N resonances (Ketchem et al., 1994). The resonance at 145 ppm is from the $N_{\epsilon 1}$ site in the indole side chain and remains unchanged upon the addition of considerable Na^+. The resonance at 184.5 ppm (7.6 kHz), however, changes by 3 ppm upon the addition of Na^+ so that 90% of the strong binding sites are occupied, and it changes by 6 ±1 ppm when 100% of the strong binding sites are occupied along with 80% of the weak binding sites. While this change is significant, it is by no means a large change, and therefore Na^+ has only a subtle effect on this site in the polypeptide backbone. ^{2}H splits the ^{15}N resonance into a 1:1:1 triplet (Figure 1B) such that the center line reflects the chemical shift frequency for the nuclear site. In these spectra the two triplets overlap significantly, but the assignment of the resonances is unambiguous. Quantitatively, the dipolar splitting can be measured from the spectra using the chemical shift values observed in Figure 1A and the outer components of the triplets. Neither the chemical shift nor the $^{15}N-^{2}H$ dipolar interaction for $N_{\epsilon 1}$ sites changes, even in the presence of a NaCl concentration corresponding to 80% double occupancy of the cation binding sites. Furthermore, only at this highest level of Na^+ occupancy is there a measurable change in the $^{15}N_{\alpha}-^{2}H$ dipolar splitting at this site.

Figure 2 shows an example of high-resolution ^{2}H NMR spectroscopy of oriented samples in the presence and absence of Na^+. Similar spectra obtained in the absence of Na^+ have recently been published (Koeppe et al., 1996). Four carbon-bound deuterons are present in this ethanolamine carboxy-terminal blocking group. In addition to four quadrupole splittings some powder pattern intensity can be observed in the spectra with the powder pattern "horns" observed at half the frequency separation of the $\nu_{||}$ components. This ambiguity is readily resolved when samples are tipped by 90° (Killian et al., 1992; data not shown); then $\Delta\nu_{obs}$ is consistent with the horns of the powder pattern and just four splittings are observed, albeit half as large. The resonance assignments have not yet been achieved for these sites due to the complexity of the local dynamics which substantially averages the quadrupolar interactions. However, it is seen that significant changes in the quadrupolar splittings occur upon Na^+ binding even at the level of 90% single occupancy.

Table 1 presents both new and previously published results on the effects of Na^+ binding on the NMR observables.

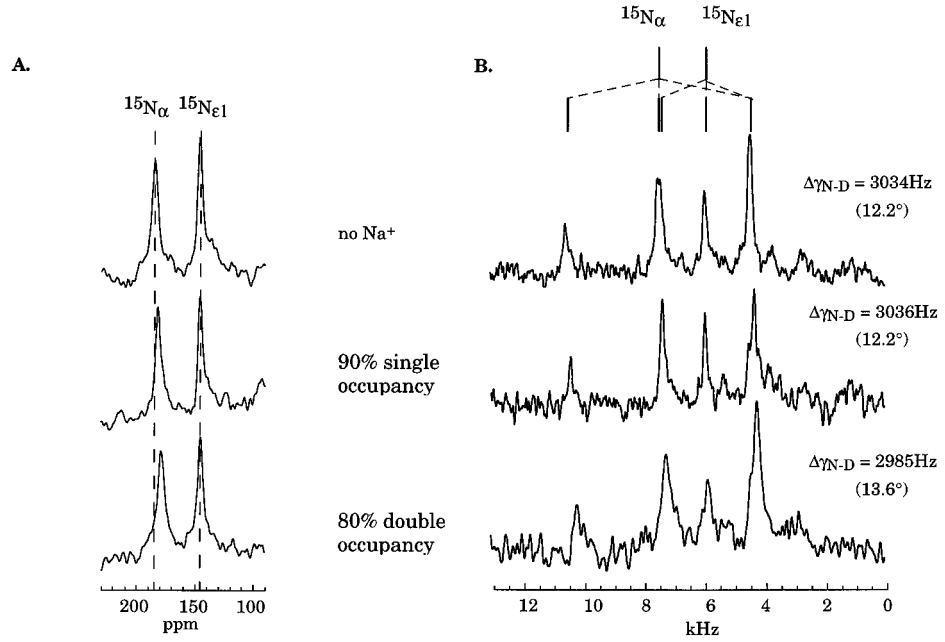

FIGURE 1: ^{15}N NMR spectra of $^{15}N_{\alpha,\epsilon1}$ Trp_{13}-labeled gramicidin A in aligned hydrated lipid bilayers with the bilayer normal parallel to B_o. The spectra were obtained at a ^{15}N frequency of 40.58 MHz using cross polarization. (A) ^1H decoupled spectra showing the anisotropic ^{15}N chemical shift for the $^{15}N_\alpha$ and $^{15}N_{\epsilon1}$ sites. Chemical shifts in the absence of cations are observed at 184.5 ppm for N_α and 145 ppm for $N_{\epsilon1}$. In the presence of Na^+ the chemical shift for $N_{\epsilon1}$ is fixed while the chemical shift for N_α changes. (B) These samples have been exchanged in D_2O, and so the spectra show the superposition of the chemical shift interaction and the $^{15}N-^2H$ dipolar interaction between spin $I = 1$ and $I = 1/2$ nuclei. The spectra are shown here on a kilohertz scale for the dipolar interaction; 7.6 and 6.0 kHz correspond to 184.5 and 145 ppm, respectively . The dipolar couplings for N_α are shown on the right as the separation of adjacent resonance components in the 1:1:1 triplet and the angular interpretation represent angles between the N−D bond and B_o.

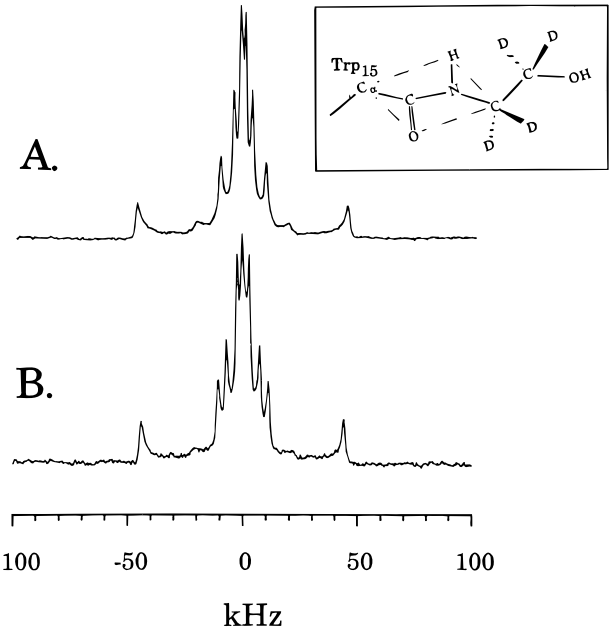

FIGURE 2: ^2H NMR spectra obtained at 61.5 MHz of ethanolamine-d_4 labeled gramicidin A in aligned hydrated lipid bilayers with the bilayer normal parallel to B_o. The quadrupole splittings are averaged by complex dynamics that have thwarted attempts to make the assignments. However, the presence of Na^+ (B) has clearly induced significant, but possibly small changes in the quadrupolar splittings as compared to the spectra taken in the absence of Na^+ (A).

While the side chains are affected only slightly by the presence of Na^+, some of the backbone data show significant changes. To quantitatively interpret these observables in the presence and absence of Na^+, the nuclear spin tensor element magnitudes and their orientation with respect to the molecular frame must be known. The chemical shift tensors used for interpreting the $^{15}N_\alpha$ and $^{13}C_1$ chemical shifts are as described by Mai et al. (1993) and Wang et al. (1992) and for $^{15}N_{\epsilon1}$ by Hu et al. (1993). For dipolar interactions the unique axis of these symmetric interaction tensors lies along the internuclear vector, and therefore, this vector or bond orientation can be determined directly from the observed dipolar splitting, $\Delta\nu_{obs}$ $(=\nu_{||}(3\cos^2\theta - 1))$. The magnitude of the $^{15}N-^2H$ dipolar interaction, $\nu_{||} = 1.6125$ kHz, is that determined from crystalline dipeptides (Hiyama et al., 1988). This model compound study showed that the N−H and N−D bond lengths were slightly different. This result is consistent with the $^{15}N-^1H$ and $^{15}N-^2H$ data obtained on the gramicidin channel and suggests that the N−D bond length is slightly longer (∼2%) than the N−H bond length.

To compare these different data types, all backbone observables have been interpreted using an assumed model for structural deformation in the gramicidin channel, in which the carbonyl oxygens rotate about the $C_\alpha-C_\alpha$ axis toward the channel axis. This is the axis about which the local motions have been shown to occur (Lazo et al., 1995). Consequently, the structural deformations are modeled as a change in the time-averaged orientation of the peptide plane pivoted about the axis joining C_α carbons in the plane. The angles in Table 1 associated with the changes in chemical shift values are calculated using the equations:

$$\sigma_{obs} = \sigma_{11}\cos^2\theta_{11} + \sigma_{22}\cos^2\theta_{22} + \sigma_{33}\cos^2\theta_{33}$$

$$\sum\cos^2\theta_{ii} = 1$$

In the absence of cations the structure is known (Table 2), and hence the angles, θ_{ii}, between the magnetic field and the chemical shift tensor are known. Therefore, a change in σ_{obs} in the presence of Na^+ with a defined model for structural deformation and with a known orientation of the

Table 1: Orientational Constraints Observed in the Absence and Presence of Na^+ at Concentrations Sufficient To Achieve 90% Single Occupancy (SO) and 80% Double Occupancy (DO) of the Channel

backbone sites[a]	chemical shift (±1 ppm)		dipolar (±40 Hz)
	$^{13}C_1$[b]	^{15}N	$^{15}N-^{2}H$
$Leu_{14}-Trp_{15}$			
$-Na^+$	−8.7	183.3	3011
90% SO	−4.7 (6°)	181.7 (1.5°)	3020 (∼0°)
80% DO		178 (5°)	3007 (∼0°)
$Trp_{13}-Leu_{14}$			
$-Na^+$	−6.7	132.8	
90% SO	−6 (∼0°)	131.5 (1°)	2165
80% DO		130.6 (2°)	
$Leu_{12}-Trp_{13}$			
$-Na^+$	−8	184.5	3034
90% SO	−4.7 (4.5°)	181.5 (4°)	3036 (∼0°)
80% DO		178.5 (7°)	2985 (1.5°)
$Trp_{11}-Leu_{12}$			
$-Na^+$	−6	134	2228
90% SO	−6.7 (∼0°)	133.5 (0.5°)	2232 (∼0°)
80% DO		132 (2°)	
$Leu_{10}-Trp_{11}$			
$-Na^+$	−6	185	3032
90% SO	0 (8.5°)	182 (6°)	
80% DO		177 (11.5°)	2840 (5°)
Trp_9-Leu_{10}			
$-Na^+$		144	
90% SO			
80% DO		145.5 (1°)	
Val_8-Trp_9			
$-Na^+$		203.5	
90% SO			
80% DO		203.8 (∼0°)	
Val_7-Val_8			
$-Na^+$	−10.7	145.8	
90% SO	−10.7 (∼0°)		
80% DO		146.3 (∼0°)	
Val_6-Val_7			
$-Na^+$		198[d]	
90% SO			
80% DO		198 (0°)[d]	
Ala_5-Val_6			
$-Na^+$			
90% SO			
80% DO			
Leu_4-Ala_5			
$-Na^+$	−8	198[d]	
90% SO	−8 (∼0°)		
80% DO		198 (0°)[d]	
Ala_3-Leu_4			
$-Na^+$	−9.3		
90% SO	−9.3 (∼0°)		
80% DO			
Gly_2-Ala_3			
$-Na^+$	−7.3	198[d]	
90% SO	−7.3 (∼0°)		
80% DO		198 (0°)[d]	
Val_1-Gly_2			
$-Na^+$		114.4	
90% SO			
80% DO		113.7 (∼0°)	
formyl $-Val_1$			
$-Na^+$		198[d]	
90% SO			
80% DO		198 (0°)[d]	

side chain sites[c]	chemical shift (±1 ppm)		quadrupolar (±1 kHz)				
	$^{13}C_{\delta 1}$[b]	^{15}N	δ_1	ϵ_3	ζ_2	ζ_3	η_2
indole$-Trp_{15}$							
$-Na^+$	−6	139					
90% SO	−6 (0°)	139 (0°)					
80% DO							
indole$-Trp_{13}$							
$-Na^+$	−2.7	145	108	32	204	−81	28
90% SO[e]	−2.7 (0°)	144 (∼0°)	110 (1°)	30 (∼0°)	206 (1°)	-82 (∼0°)	26 (∼0°)
80% DO							
indole$-Trp_{11}$							
$-Na^+$	−2	144	77	43	192	−99	39
90% SO[e]	−2 (0°)	144 (0°)	83 (1°)	44 (∼0°)	198 (2°)	−102 (1°)	39 (0°)
80% DO		144 (0°)					
indole$-Trp_9$							
$-Na^+$	5.3	145					
90% SO	5.3 (0°)	145 (0°)					
80% DO							

Table 1 (Continued)

terminal blocking group	quadrupolar (±1 kHz)[f]			
	A	B	C	D
ethanolamine				
$-Na^+$	91.2	19.5	7.9	3.7
90% SO	88.0	21.7	14.4	5.2
80% DO				

[a] Angles in parentheses are calculated as a change in time-averaged orientation about the $C_\alpha-C_\alpha$ axis. [b] Data are from Smith et al. (1990) and Separovic et al. (1994) using 0.16 M NaCl, and since these authors have prepared samples with a molar concentration of gramicidin that is approximately half of what we have used, the Na^+ occupancy is slightly greater than 90% single occupancy. Data were reported in the literature as chemical shift anisotropy (CSA) and are reported here as values of $\sigma_{||}$ (=0.67 × CSA). The uncertainty in the data for CSA was reported as ±2 ppm, which is equivalent to ±1.3 ppm for the $\sigma_{||}$ presented here. [c] Angles calculated as a change in time-averaged orientations with respect to B_0. [d] Observed as a single resonance in $^{15}N_{1,3,5,7}$-labeled gramicidin A. [e] For the ^2H and ^{15}N data 0.6 M NaCl was used, implying a somewhat greater occupancy than 90% single occupancy. [f] Quadrupolar splitting observed for the four carbon-bound deuterons in the ethanolamine group.

Table 2: Torsion Angles for the Structural Model Used for the Calculation of Deformation Angles[a]

residue	ϕ	ψ	ω	χ_1	χ_2	χ_3
Val_1	−107.66	120.58	171.28	177.44		
Gly_2	151.13	−129.35	176.09			
Ala_3	−114.83	143.93	−174.09			
Leu_4	121.58	−135.93	−173.31	−157.28	151.92	
Ala_5	−116.08	124.83	−178.79			
Val_6	146.7	−118.17	176.16	58.90		
Val_7	−120.19	125.72	164.60	−151.41		
Val_8	151.68	−120.34	177.77	60.42		
Trp_9	−110.55	128.31	−173.03	−74.17	−81.81	171.03
Leu_{10}	129.24	−128.14	176.29	−72.61	−70.72	
Trp_{11}	−108.76	151.52	168.2	−70.63	−90.81	−173.86
Leu_{12}	114.43	−119.08	174.6	−176.82	−59.47	
Trp_{13}	−99.98	153.38	167.11	−63.75	−85.09	175.97
Leu_{14}	111.18	−115.44	178.48	−176.07	−71.77	
Trp_{15}	−108.46	127.38	−177.86	−60.64	−90.06	175.96

[a] Ketchem, Roux, and Cross, unpublished results.

chemical shift tensor with respect to the structural deformation axis leads to an angle of rotation about the $C_\alpha-C_\alpha$ axis. Similarly, deformation angles can be calculated on the basis of the changes in the dipolar interactions. Furthermore, the spectra of the gramicidin dimer represent the time average of both monomers. Therefore, with single occupancy, the observed data and interpreted deformation angles represent the average of occupied and unoccupied monomer structures. Consequently, the double occupancy data represent a more accurate view of the cation influence on structure. However, angles from both chemical shifts and dipolar interactions represent maximal structural deformation, since they do not take into account other possible interpretations of the changes in the nuclear spin interaction observables.

DISCUSSION

The data in Table 1 show that when NaCl solution is used to hydrate gramicidin A/lipid preparations, only local effects on the gramicidin A channel are observed. The side chains are largely unaffected, but there are small changes in the ^2H quadrupolar splittings for some of the indole deuterons. The fact that some of these changes represent an increase in quadrupole splitting upon cation binding means that there is no change in the global orientation of the channel with respect to the lipid bilayer. Because the motionally averaged tensors are all aligned so that the unique axis is parallel to the global motional axis, which is the bilayer normal, an increase in the observed nuclear spin interaction magnitude would either mean a change in the local orientation of the ring with respect to the field or a decreased angle between the global motional axis and the magnetic field. This angle is 0° without Na^+ present (Fields et al., 1988), and therefore the small changes in orientation must reflect local changes. This is confirmed by the lack of significant changes induced by Na^+ in the nuclear spin interactions for all sites in the polypeptide backbone except for the peptide planes of $Leu_{14}-Trp_{15}$, $Leu_{12}-Trp_{13}$, $Leu_{10}-Trp_{11}$, and the ethanolamine blocking group.

There are three plausible explanations for the changes in observed chemical shifts. A change in orientation of the interaction tensor with respect to the field due to a change in structure will alter the value of the observables (Smith et al., 1990; Ketchem et al., 1994; Separovic et al., 1994). Similarly, a change in dynamic amplitudes that lead to a different time averaging of the spin interaction tensors will also alter the value of the observables (Cross, 1994). A third possibility is that the electron density around the observed nucleus could change as a result of cation binding, causing a change in the tensor element magnitudes or tensor element orientations with respect to the molecular frame (Wang & Ellis, 1991). While chemical shift interactions are particularly sensitive to such changes in electron density, dipolar interactions are less sensitive.

Changes in both ^{15}N and $^{13}C_1$ chemical shifts suggest the possibility of significant structural or dynamic changes for a few peptide planes, while the $^{15}N_\alpha-^2H$ dipolar interactions suggest neither for these same sites. Clearly the deformation model used in the Results section is not the complete story, because no one deformation amplitude for each peptide plane is consistent with all of the data for that plane. The deformation amplitudes are different as determined by ^{15}N and ^{13}C chemical shifts in a single peptide plane. Therefore,

we could consider a change in the ω torsion angle; in this way different amplitudes on either side of the peptide bond could be used. However, this does not take into account the $^{15}N-^{2}H$ dipolar results which are from the same side of the peptide bond as the ^{15}N chemical shift. Consequently, a change in the ω torsion angle does not account for all of the experimental observations. In fact, there does not appear to be any reasonable deformation or motional averaging model that accounts for these observations. In part, this is due to the near alignment of the unique axis of the dipolar interaction tensor and the dominant ^{15}N chemical shift tensor element. In other words, it is difficult to develop a model that avoids influencing the $^{15}N-^{2}H$ dipolar interaction while significantly affecting the ^{15}N chemical shift. Instead, a general trend can be described in which the $^{13}C_1$ chemical shift is influenced the most, the ^{15}N chemical shift, intermediate, and the $^{15}N-^{2}H$ dipolar interaction, the least. Such a gradient is qualitatively consistent with indirect polarization resulting from ion-induced polarization of the carbonyl oxygens that solvate the cations in the channel binding site. Polarization induced by cations on a catalytic surface has been experimentally characterized (Wang & Ellis, 1991). Moreover, computational efforts to account for K^+ binding energetics and ion selectivity in valinomycin, an ion carrier, suggest substantially increased partial charges on the carbonyl oxygens (Aqvist et al., 1992). Such changes in electron density would result from ion-induced polarization effects. Here we propose that a change in electron density at the oxygen is alleviated by a gradient of electron density changes, greatest at the carbonyl carbon and less at the amide ^{15}N site as reflected by changes in the chemical shift observables. But while the chemical shift tensor elements reflect the electron densities of the observed nuclei the dipolar interaction is influenced to a lesser extent, and moreover the $^{15}N-^{2}H$ dipolar interaction is even further removed from the electrostatic interaction between the carbonyl oxygen and the cation.

Based on this complete analysis of all of the NMR data and with the exception of the $Leu_{10}-Trp_{11}$ peptide plane, there appears to be no significant change in polypeptide structure even at the highest cation loading of the channel. For this Leu_{10} carbonyl site the dipolar data are consistent with a 5° rotation of the carbonyl toward the channel axis, but even here it is possible that the change in dipolar splitting is the result of an increase in dynamic amplitude, which would reduce the magnitude of the time-averaged interaction. Or, it is possible that this large effect is the result of an even larger electron density change that influences the $^{15}N-^{2}H$ bond length and hence the static dipolar interaction magnitude. Such cation-induced bond length changes have been observed in an NMR study of a Cs^+-promoted silver catalyst (Wang & Ellis, 1991). We suggest that for those sites which show a significant difference in chemical shift, but not in the dipolar data, the chemical shift tensor has changed as a result of polarization due to Na^+ binding. A direct polarization effect on the $^{13}C_1$ and ^{15}N sites is ruled out because nitrogens, such as those of Leu_{10} and Leu_{12}, are unaffected by Na^+ despite their close proximity to the cation that is interacting with the Leu_{10} carbonyl oxygen, the favored site for Na^+ binding. As seen in Figure 3 only those nitrogens that are in the same peptide plane with the affected carbonyl carbons are influenced by Na^+ binding. Nitrogens in neighboring peptide planes are unaffected. Furthermore, the only peptide planes influenced by Na^+ are those near the channel mouth and C-terminus of the polypeptide with the carbonyl oxygen oriented toward the bilayer surface. Therefore, it appears that by binding to the carbonyl oxygen, Na^+ has indirectly polarized, by through-bond effects, the C_1 and N_α atoms of the peptide planes. This result elevates the importance of polarizability effects for molecular dynamics studies, as has recently been noted by Roux et al. (1995).

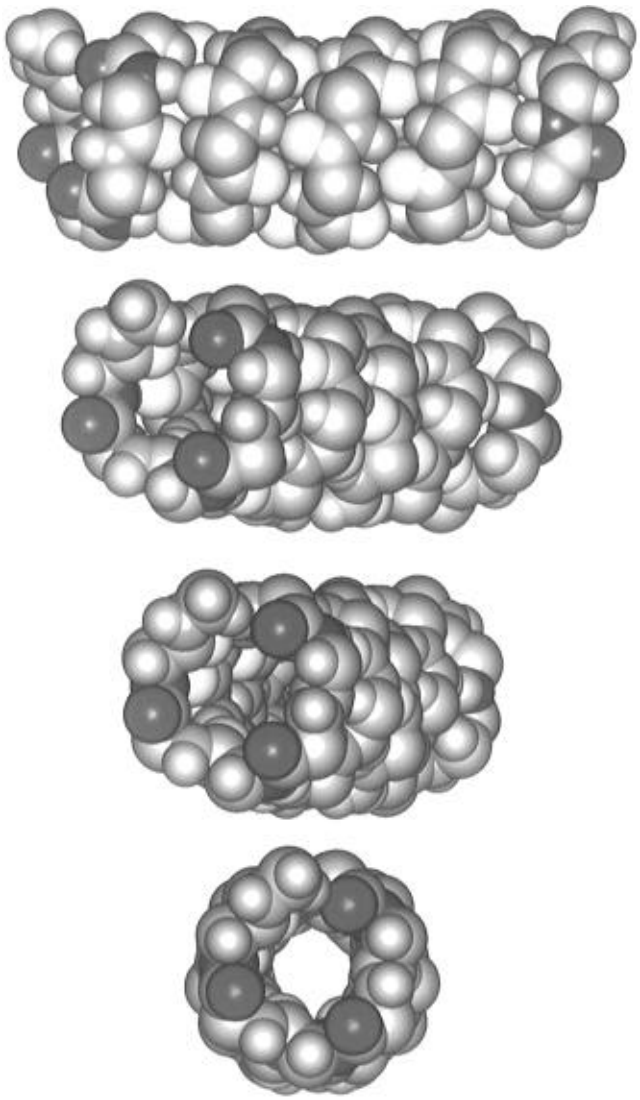

FIGURE 3: Refined backbone structure of the gramicidin channel in four views varying from the end to side views. Red identifies the carbonyl oxygens and blue the amide nitrogens. Only the carbonyl chemical shifts of residues 10, 12, and 14 are affected (deep red) by the presence of Na^+ in the channel. The other $^{13}C_1$ sites show no change in chemical shift and are represented in pink. Only the amide ^{15}N chemical shifts of residues 11, 13, and 15 are affected (dark blue) by Na^+, and the other ^{15}N sites are represented by a light shade of blue. The ethanolamine is only partially represented (the methoxy group is missing) at the C-terminus, because its structure is incompletely defined. The ethanolamine which is in the vicinity of the Leu_{10} carbonyl is almost certainly involved in the solvation of Na^+ in its binding site.

Gramicidin facilitates cation conductance by lowering the energy barrier for cation passage across membranes. Even so, most of the waters of hydration are stripped from the cation as it enters the channel, and therefore, the channel must replace this solvation environment so that a large potential energy barrier is not formed at the channel entrance. Neither should the solvation of the cation be optimal, because

strong cation binding or the development of a deep potential energy well along the conductance pathway would hinder conductance. The observed binding constant is 37 M^{-1}, reflecting a relatively weak binding site but still adequate for attracting cations from outside the channel (Chiu & Jakobsson, 1989). The absence of structural deformation is consistent with a relatively weak binding site. Correlations between the influence of cation binding on protein structure and functional roles in Ca^{2+} binding proteins have recently been suggested (Skelton et al., 1994). For regulatory Ca^{2+} binding sites, strong binding and deformation are induced upon cation binding to provide a response mechanism for this secondary messenger function. Other Ca^{2+} binding proteins are involved in Ca^{2+} uptake, transport through the cell, and Ca^{2+} homeostasis. For calbindin, a calcium binding protein, this "buffering" activity induces very little structural deformation upon Ca^{2+} binding. In essence Ca^{2+} is binding to a "preformed" binding site (Skelton et al., 1994). Gramicidin appears to show a similar functional response to cation binding for monovalent cations. The binding of Na^+ to the channel provides sufficient energy to make up for its loss in hydration energy, but the binding is not so strong that high conductance cannot be achieved. In fact, Na^+ appears to be binding to "preformed" binding sites in the channel. While the backbone is dynamic, the arrangement of channel atoms in the absence of Na^+ is as good as can be achieved within reasonable energetic limits for solvating Na^+. This is not to say that the binding site is ideal but that deforming the backbone structure within the energetic boundaries of the potential energy surface does not generate a better conformation for binding Na^+. This is contrary to the regulatory binding of monovalent cations by dialkylglycine dicarboxylase which is activated by K^+ and deactivated by Na^+ (Miller, 1993; Toney et al., 1993). This protein changes structure substantially upon cation binding.

The rate-limiting step for conductance is the barrier at the bilayer center rather than at the bilayer surface (Hu & Cross, 1995), and therefore, the solvation environment for Na^+ in the gramicidin channel is adequate to prevent a rate-limiting barrier at the channel entrance. The lack of structural deformation in the time-averaged structure, despite the backbone flexibility, suggests that the contributions to the cation environment from the polypeptide are dominated by a maximum of just two carbonyl oxygens at any one time. Models for the solvation that utilized relatively large local deformations and that had identified three or four carbonyls that simultaneously contribute to the cation solvation environment appear to be incorrect, but others with an off-axis cationic pathway and with just two carbonyls dominating the solvation environment are supported by this study. The helix shown in Figure 4 emphasizes the carbonyl oxygens for their role in this off-axis path for the cations. It has been suggested that cation selectivity in the proteinaceous channels results from differences in the solvation environment within the channel for various cations (Eisenman & Horn, 1983; Simon et al., 1973). For gramicidin, such a mechanism could be achieved because the binding site is not deformable or plastic, and so cations of larger size will interact with more carbonyl oxygens at any one time and hence their solvation environment will be quite different from the environment for the smaller cations.

FIGURE 4: Side view of the refined gramicidin channel showing the helical array of carbonyl oxygens (red). Since the cation passes through the channel off axis, it will follow this path of carbonyl dipoles that are essential for its solvation in the channel.

ACKNOWLEDGMENT

The authors thank Francis Separovic, Paul Ellis, Benoit Roux, and Walter Chazin for helpful discussions. The authors are indebted to the staff of the FSU NMR Facility: J. Vaughn, R. Rosanske, and T. Gedris for their skillful maintenance and service of the NMR spectrometers and H. Henricks and U. Goli in the Bioanalytical Synthesis and Services Facility for their expertise and maintenance of the ABI 430A peptide synthesizer and HPLC equipment.

REFERENCES

Akutsu, H., & Seelig, J. (1981) *Biochemistry 20*, 7366−7373.
Andersen, O. S. (1984) *Annu. Rev. Physiol. 46*, 531−548.
Aqvist, J., & Warshel, A. (1989) *Biophys. J. 56*, 171−182.
Aqvist, J., Alvarez, O., & Eisenman, G. (1992) in *Membrane Proteins: Structures, Interactions and Models* (Pullman, A., Jortner, J., & Pullman, B., Eds.) pp 367−382, Kluwer Academic Publishers, Boston, MA.
Badger, J., Kapulsky, A., Gursky, O., Bhyravbhatia,B., & Caspar, D. L. D. (1994) *Biophys. J. 66*, 286−292.
Chiu, S.-W., & Jakobsson, E. (1989) *Biophys. J. 55*, 147−157.
Chiu, S.-W., Subramaniam, S., Jakobsson, E., & McCammon, J. A. (1989) *Biophys. J. 56*, 253−261.
Chiu, S.-W., Jakobsson, E., Subramaniam, S., & McCammon, J. A. (1991) *Biophys. J. 60*, 273−285.
Cross, T. A. (1994) *Annu. Rep. NMR Spectrosc. 29*, 123−167.
Eisenman, G., & Horn, R. (1983) *J. Membr. Biol. 76*, 196−225.
Elber, R., Chen, D. P., Rojewska, D., & Eisenberg, R. (1995) *Biophys. J. 68*, 906−924.
Fields, G. B., Fields, C. G., Petefish, J., Van Wart, H. E., & Cross, T. A. (1988) *Proc. Natl. Acad. Sci. U.S.A. 85*, 1384−1388.
Fields, C. G., Fields, G. B., Noble, R. L., & Cross, T. A. (1989) *Int. J. Pept. Protein Res. 33*, 298−303.
Fischer, W., & Brickmann, J. (1983) *Biophys. Chem. 18*, 323−337.
Hinton, J. F., Whaley, W. L., Shungu, D., Koeppe, R. E., Jr., & Millett, F. S. (1986) *Biophys. J. 50*, 539−544.
Hiyama, Y., Niu, C.-H., Silverton, J. V., Bavoso, A., & Torchia, D. A. (1988) *J. Am. Chem. Soc. 110*, 2378−2383.
Hu, W., & Cross, T. A. (1995) *Biochemistry 34*, 14147−14155.
Hu, W., Lee, K.-C., & Cross, T. A. (1993) *Biochemistry 32*, 7035−7047.

Hu, W., Lazo, N. D., & Cross, T. A. (1995) *Biochemistry 34*, 14138−14146.
Jordan, P. C. (1990) *Biophys. J. 58*, 1133−1156.
Ketchem, R. R., Hu, W., & Cross, T. A. (1993) *Science 261*, 1457−1460.
Ketchem, R. R., Hu, W., Tian, F., & Cross, T. A. (1994) *Structure 2*, 699−701.
Ketchem, R. R., Roux, B., & Cross, T. A. (1996) in *Biological Membranes: A Molecular Perspective from Computation and Experiment* (Merz, K. M., & Roux, B., Eds.) pp 299−322, Birkhauser, Boston, MA.
Killian, J. A., Taylor, M. J., & Koeppe, R. E., II (1992) *Biochemistry 31*, 11283−11290.
Koeppe, R. E., II, Vogt, T. C. B., Greathouse, D. V., Killian, J. A., & de Kruijff, B. (1996) *Biochemistry 35*, 3641−3648.
Lazo, N. D., Hu, W., & Cross, T. A. (1995) *J. Magn. Reson. 107B*, 43−50.
Mackay, D. H., Berens, P. H., Wilson, K. R., & Hagler, A. T. (1984) *Biophys. J. 56*, 229−248.
Mai, W., Hu, W., Wang, C., & Cross, T. A. (1993) *Protein Sci. 2*, 532−542.
Miller, C. (1993) *Science 261*, 1692−1693.
North, C. L., & Cross, T. A. (1995) *Biochemistry 34*, 5883−5895.
Olah, G. A., Huang, H. W., Liu, W., & Wu, Y. (1991) *J. Mol. Biol. 218*, 847−858.
Roux, B. (1993) *Chem. Phys. Lett. 212*, 231−240.
Roux, B., & Karplus, M. (1991) *Biophys. J. 59*, 961−981.
Roux, B., & Karplus, M. (1993) *J. Am. Chem. Soc. 115*, 3250−3262.
Roux, B., & Karplus, M. (1994) *Annu. Rev. Biophys. Biomol. Struct. 23*, 731−761.
Roux, B., Prod'hom, B., & Karplus, M. (1995) *Biophys. J. 68*, 876−892.
Separovic, F., Gehrmann, J., Milne, T., Cornell, B. A., Lin, S. Y., & Smith, R. (1994) *Biophys. J. 67*, 1495−1500.
Simon, W., Morf, W. E., & Meier, P. C. (1973) *Struct. Bonding (Berlin) 16*, 113−160.
Skelton, N. J., Kordel, J., Akke, M., Forsen, S., & Chazin, W. J. (1994) *Struct. Biol. 1*, 239−245.
Skerra, A., & Brickmann, J. (1987) *Biophys. J. 51*, 969−976.
Smith, R., Thomas, D. E., Atkins, A. R., Separovic, F., & Cornell, B. A. (1990) *Biochim. Biophys. Acta 1026*, 161−166.
Toney, M. D., Hohenester, E., Cowan, S. W., & Jansonius, J. N. (1993) *Science 261*, 756−759.
Urry, D. W. (1971) *Proc. Natl. Acad. Sci. U.S.A. 68*, 672−676.
Urry, D. W. (1975) *Int. J. Quantum Chem.: Quantum Biol. Symp. 2*, 221−235.
Urry, D. W., Prasad, K. U., & Trapane, T. L. (1982) *Proc. Natl. Acad. Sci. U.S.A. 79*, 390−394.
Venkatchalam, C. M., & Urry, D. W. (1984) *Comput. Chem. 5*, 64−71.
Wang, C., Teng, Q., & Cross, T. A. (1992) *Biophys. J. 61*, 1550−1556.
Wang, X., & Ellis, P. D. (1991) *J. Am. Chem. Soc. 113*, 9675−9676.
Woolf, T. B., & Roux, B. (1994) *Proc. Natl. Acad. Sci. U.S.A. 91*, 11631−11635.

BI961170K